Proceedings of the ASME 2018
Dynamic Systems and Control Conference
DSCC2018
September 30-October 3, 2018, Atlanta, Georgia, USA

DSCC2018-8978

LATENT VARIABLE GRASP PREDICTION FOR EXOSKELETAL GLOVE CONTROL

Raghuraj J. Chauhan
Robotics and Mechatronics Lab
Department of Mechanical Engineering
Virginia Tech
Blacksburg, VA 24060
Email: raghur1@vt.edu

Pinhas Ben-Tzvi
Robotics and Mechatronics Lab
Department of Mechanical Engineering
Virginia Tech
Blacksburg, VA 24060
Email: bentzvi@vt.edu

ABSTRACT

This paper presents a grasp prediction algorithm designed to govern the motion of an exoskeletal glove in rehabilitative and assistive applications. Recent research into the dynamics of hand motion has shown that the complex motion of the finger joints can be represented as a smaller set of coordinated motions or latent variables. This fact forms the basis of the proposed algorithm capable of successful prediction even with noisy data. From relatively small motion (minute user hand movements) as the input, the developed algorithm can predict intended grasp configurations. The 16 finger joint angles, with random noise, are mapped onto a set of six latent variables for which the estimated noise and future configuration are simultaneously determined using a linear regression. The algorithm was tested in simulation on published motion data from 30 healthy subjects performing a set of common grasps on multiple objects. The algorithm was able to determine the target state with an accuracy of approximately 90% for each subject, despite the nonlinear motion and non-uniform trajectory variations. We propose that the predicted grasp is an adequate target for an exoskeletal glove to provide initial gross movement for the user, then iteratively converge to the desired grasp with only limited additional user input.

NOMENCLATURE

$\vec{\theta}, \vec{\theta}'$	Original and reconstructed hand pose
n	Hand degrees of freedom
$\boldsymbol{W}$	Principal component matrix
p	Number of principal components
$\vec{\lambda}$	Principal component weights
$\vec{\phi}$	Reduced variable hand pose
$\vec{\psi}$	Extrapolated reduced variable hand pose
$\vec{\beta}, b_{j,k}$	Pose regression slopes and intercepts
τ^-, τ^+	Look back and look ahead distanced
ζ, τ_0^-	Look back tuning parameters
s_i, c_i	Prediction score and confidence
γ	Score tuning parameters
α, μ, σ	Confidence tuning parameter
$\tilde{\theta}, \epsilon$	Noisy joint angle and noise
$f_{out}, f_{user}, f_{\psi}$	Glove, user, and algorithm forces
ν, ω	Haptic authority gains

1 INTRODUCTION

The continual developments in novel exoskeletal glove design over the last decade have been accompanied by an increase in the modeling and characterization of human grasping. The pose of the human hand, when performing a grasp, is defined by 21 degrees of freedom that correspond to the finger joints [1]. It has been shown that this 21-dimensional space can be mapped to one of lower dimensionality based on the coordinated motion of the finger joints using Principal Component Analysis (PCA) [2] or Gaussian Process Latent Variable Mapping (GPLVM) [3]. This lower dimensional space has been used to control fully robotic hands to perform common grasps as defined by the Feix taxonomy [4] on ordinary objects in [5, 6] but has not yet been applied to an exoskeletal system.

Many of the designs for exoskeletal gloves rely on the use of soft robotics and rigid mechanisms that extensively couple

the finger joints and reduce the effective degrees of freedom in the system [7–9]. As a result, these devices can only operate through binary movement of the finger joints, collectively flexing or extending them. The motion between finger joints has been well studied and there is a definite degree of independence between the metacarpophalangeal joint (MCP) and proximal interphalangeal joint (PIP) along each finger [2,10,11] while performing activities of daily living (ADLs). It has been shown that for the unconstrained motion of the fingers, motion in the distal interphalangeal joint (DIP) joint is highly correlated to motion in the PIP joint [10]. By mechanically coupling these joints, the capability to perform the required independent joint motions is sacrificed in order to achieve a simpler mechanical design. We, however, believe that there is a need to actuate and control these independent joints in an exoskeletal glove so a user can perform all ADLs. This work seeks to provide the control framework for commanding the motion of such a glove using PCA.

The PCA method has been used to reduce noise in data [12]. It has therefore shown to be a useful means by which to extract the intended hand trajectory of an operator despite noisy or vestigial measurements [13]. We assume that most of the noise is captured by the exclusion of the higher order principal components. By performing this dimensional reduction, followed by a linear regression, the intended hand pose is extracted, used to command the gross input of the glove and guide the user towards their desired position. These hand poses have been described by the GRASP taxonomy.

The GRASP taxonomy presented by Feix et al (2016) in [4] merges previous taxonomies of common grasps and provides a framework for grouping these grasps based on the hand geometry exhibited. We direct the reader to this work to understand the grasp names and numbers used here. The work by Romero et al (2010) in [3] shows a clear grouping or clustering of grasps in the lower dimension manifold as well. This grouping is broader but also includes the spatiotemporal characteristics of the grasps. We later discuss how these characteristics are significant to the prediction algorithm.

The prediction algorithm was tested on the HUST dataset [14]. The experiment used to compile the dataset had 30 healthy subjects (15 male and 15 female) perform the 33 grasps defined by the Feix taxonomy. The test for each grasp consisted of grasping three different objects appropriate for that grasp three times each, resulting in a total of 8910 total trials. All of the finger joint angles were measured for each subject, excluding the adduction of the fingers save the thumb. This resulted in a 16 degree of freedom (DOF) representation of the pose of the hand. The data was recorded with timestamps from the start of the trial, with the hand in a neutral position, to the end of the trial with the hand performing the grasp.

This work builds on previous characterizations of grasping via PCA that only group and model the grasps in their final configurations [2,5,10]. We present a novel prediction algorithm that uses PCA during the movement towards the final grasp configuration to predict the intended grasp of the user. This algorithm can then be applied to a haptic controller to guide the user's motion towards their intended grasp, even when they are unable to fully do so under their own power.

2 PREDICTION ALGORITHM

Although we will provide a brief formulation of the PCA used in this work, we refer the reader to [2] for a generalized visualization of the resulting principal components. The PCA mapping is applied to noisy data in the joint space of the hand and the trajectory is extrapolated to find the predicted grasp using a heuristic scoring function. The validity of the prediction is determined based on the functional and geometric relationship between predicted and target grasps which will be described later in Section 3.

2.1 PCA and Dimensional Reduction

The pose of a hand is defined as

$$\vec{\theta} = \{\theta_1, \theta_2, \dots, \theta_n\} \tag{1}$$

where θ_i is the i^{th} joint angle of the fingers on the hand.

The final grasp poses, $\vec{\theta}$, for each trial are stored in $\boldsymbol{X}$ as shown in Eqn. (2) on a per subject basis and then each column is centered around the mean for that θ_i. The resulting design matrix is

$$\boldsymbol{X} = \begin{bmatrix} \vec{\theta}_1 \\ \vec{\theta}_2 \\ \cdot \\ \cdot \\ \cdot \\ \vec{\theta}_n \end{bmatrix} \in \mathbb{R}^{m \times n} \tag{2}$$

where m is the number of trials per subject and n is the number of hand DOFs considered per subject. To represent the fully defined hand $n = 21$ [1], but in the case of the HUST dataset, $n = 16$ due to the exclusion of the non-thumb adduction and the thumb MCP joint being resolved as a single angle. For our purposes, we use $n = 12$ to include only the adduction of the thumb and the MCP and PIP joints of the remaining fingers. The coupling between the PIP and DIP joints means that only using the PIP joints for mapping and prediction during unimpeded motion is sufficient. Thumb adduction is a primary classifier for grasp differentiation and is, therefore, the only thumb joint necessary in [15]. Initial experiments with the algorithm described in this work showed little improvement due to the inclusion of additional thumb joints.

From the covariance of the design matrix, $\boldsymbol{X^T X}$, the eigenvectors and their respective eigenvalues are extracted using

$$\boldsymbol{W} = \{PC_1, PC_2, \dots, PC_p\} \tag{3}$$

$$\vec{\lambda} = \frac{\{\lambda_1, \lambda_2, \dots, \lambda_p\}}{\sum_{k=1}^{p} \lambda_k} \tag{4}$$

$$\vec{\phi} = \vec{\theta}\boldsymbol{W} \tag{5}$$

$$\vec{\theta}' = \boldsymbol{W}^T \vec{\phi} \tag{6}$$

such that $\boldsymbol{\lambda_1}$ is the largest eigenvalue of $\boldsymbol{X^T X}$ and $\boldsymbol{PC_1}$ is its corresponding eigenvector or principal component. $\boldsymbol{W}$ is the matrix of the principal components of $\boldsymbol{X}$. The value of p is chosen so the p largest principal components together capture more than 95% of the variance in the grasp configurations. To maintain consistency between all the subjects, the p = 6 was used. The process for determining the reconstructed pose, $\vec{\boldsymbol{\theta}}'$, after being projected into $\vec{\boldsymbol{\phi}}$, the lower dimensional space, is shown in Eqn. (6). The effects of the using an increasing number of principal components on the fidelity of the projection and reconstruction of a grasp are shown in Fig. 1.

2.2 Mapping and Prediction

The reduced variable hand pose over time is fit to a line and projected forward in time to extrapolate a future pose based on the current geometry using

$$\vec{\psi}(t) = \vec{\phi}(t) + \vec{\beta}(t)\tau_t^+ \tag{7}$$

where $\vec{\psi}(t)$ is the extrapolated pose, $\vec{\phi}(t)$ is the current pose, $\vec{\beta}(t)$ is the vector of slopes of the lines of best fit for each principal component, and τ_t^+ is the distance forward in time to extrapolate. The amount of data used to perform the linear regression at the next time step is determined using Eqn. (8) so that $\tau_{i,t+1}^-$ decreases as the slope of the line increases. This stemmed from the observation that high principal component magnitude slopes, β_i, sometimes indicated that nonlinear movements were imminent. Since the shape of the trajectory is unknown, using a smaller amount of prior data allows the extrapolation to react more quickly.

$$\tau_{i,t+1}^- = \tau_0^-(1 + \left|1 - \zeta\beta_{i(t)}\right|) \tag{8}$$

The values of τ_0^- and ζ are tuned parameters and β_i is the slope of the line of best fit for the trajectory of $\vec{\phi}_i$.

The identical forward time projection distance for the regression line of each principal component at the next time step, τ_{t+1}^+, is determined by Eqn. (9).

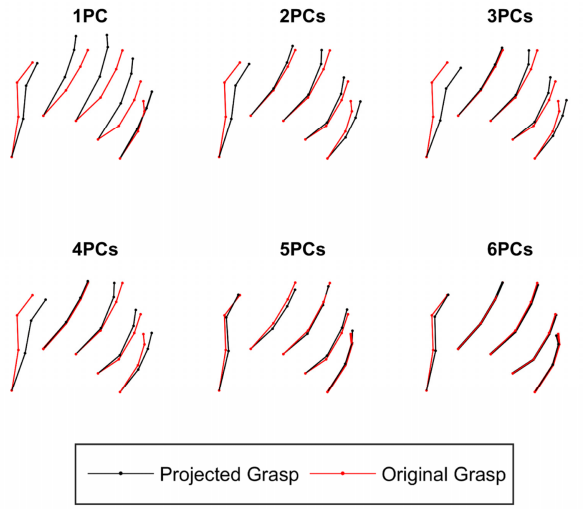

Figure 1: Reconstruction of Grasp 10, Power Disk, using an increasing number of principal components. The reconstructed pose matches the original pose more closely as more principal components are used in the reconstruction.

$$\tau_{t+1}^+ = \frac{\sum_{j=1}^{g} \min_{\tau_{t+1}^+ \in \mathbb{R}} \left[\sum_{k=1}^{p} \frac{\left|\beta_k(t)\tau_{t+1}^+ - \phi_k + b_{j,k}\right|}{p\sqrt{\beta_k(t)^2 + 1}} \right]}{g} \tag{9}$$

It is determined as the mean value, between g possible grasp configurations, that collectively minimizes the distance between each principal component configuration $\vec{\phi}$ and its respective line defined by Eqn. (7). The known magnitude of the principal component configuration at the start of motion for each grasp is $b_{j,k}$. The subscripts j and k indicate iteration through the grasp configurations and principal components, respectively. The computational requirements for calculating τ_{t+1}^+ are reduced by evaluating Eqn. (9) once every several iterations of the algorithm. Further performance improvement is achieved by looking only at the most representative grasp in each group in Tab. 2 rather than all the grasps in the Feix taxonomy. In this case, g = 8 rather than g = 33 in Eqn. (9).

The most pivotal part of the process is the actual selection of the future pose. In many cases, motion towards several grasps looks similar. To overcome this, we implement the following equations to determine the most likely grasp.

$$s_i(t) = \sum_{k=1}^{p} \lambda_k \left| \frac{\left(\phi_{i,k} - \psi_k(t)\right)^\gamma}{\phi_{i,k}} \right| \tag{10}$$

$$c_i(t) = \int_{t_0}^{t} \alpha(1 - s_i(t) - \mu)^\sigma dt \tag{11}$$

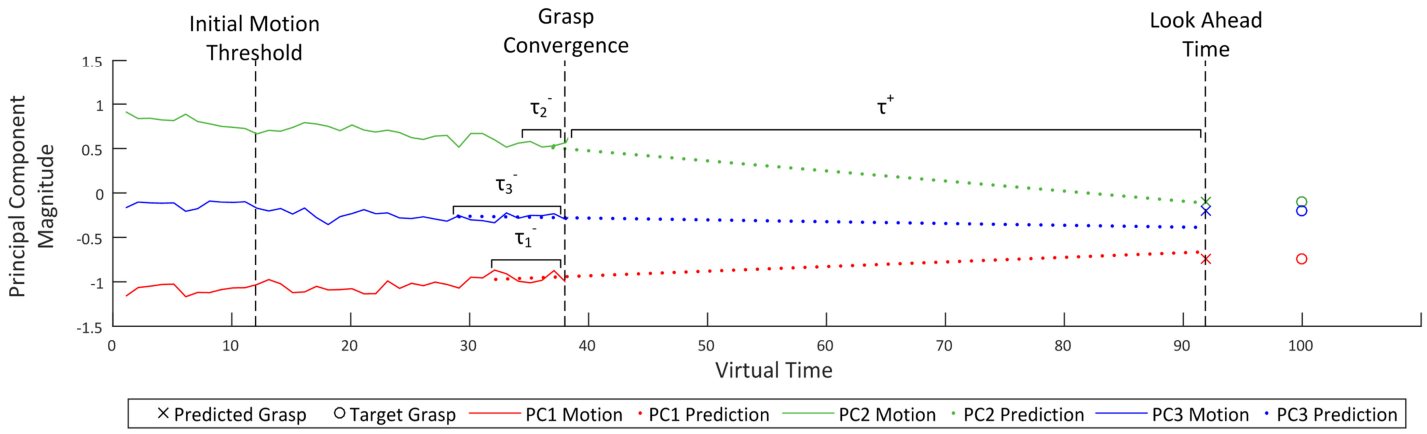

Figure 2: The motion for Grasp 13, Precision Sphere. The algorithm uses six principal components but only three are shown for clarity.

The values $s_i(t)$ and $c_i(t)$ are respectively the score and confidence for the selection of each of the 33 grasps in the Feix taxonomy as the predicted pose. The determination of $s_i(t)$ is such that the percent error for each principal component forms a weighted average based on the eigenvalue or dominance, λ_k, for that principal component as well as the magnitude of the error for that component using the exponent γ. The confidence is evaluated so that a certain tuned confidence parameter of μ must be exceeded for the value of $c_i(t)$ to increase. The parameters α and σ are heuristic tuning parameters that influence the confidence so that a continuous low score correlates to a greater confidence for the i^{th} grasp. It should be noted that based on this formulation, a lower score indicates a better match. The predicted pose is determined once $c_i(t)$ exceeds the predefined threshold for any grasp. To ensure that the required motion to predict the grasp was accurate given the irregular resting times of the subject prior to actually beginning the grasp, the fitting did not begin until a certain threshold of movement was exceeded. This delay is only useful for defining a metric by which to evaluate the algorithm and would not need to exist in an actual implementation.

3 EXPERIMENTAL RESULTS

As previously stated, the algorithm was tested on the HUST dataset with the data modified through the injection of random noise, ϵ, as shown by Eqn. (12).

$$\tilde{\theta}_i = \theta_i + \epsilon;\ -5° \leq \epsilon \leq 5° \qquad (12)$$

Each trial in the dataset begins with the subject keeping their hand in a neutral resting position and ends once they complete the specified grasp.

The prediction accuracy and percent of the grasp trajectory necessary for the prediction were measured for three simulations of the prediction algorithm per trial, per object, per grasp in the dataset and are presented in Tab. 1. The accuracy of the grasp is defined as the fulfillment of any of the following criteria:

Table 1: Performance results for all subjects.

	Accuracy (%)		Motion Required (%)	
	Mean	Std. Dev	Mean	Std. Dev
Females	77.93	10.78	25.86	3.62
Males	79.59	10.79	26.72	4.80

Table 2: Grasp groupings.

Group	Grasp Number(s)
Cylindrical Wrap	1, 2, 3
Sphere	11, 13, 14, 26, 27, 28
Two Finger Pinch	9, 24, 31, 33
Prismatic Small Stick	6, 7, 8, 20, 25, 21, 23
Index Extension Wrap	17, 19, 29, 32
Disk	10, 12
Flat Parallel	18, 22
Adducted Thumb Wrap	4, 5, 15, 16, 30

a) The predicted and target grasp are the same
b) The predicted and target grasp fall under the same category according to Tab. 2. Visual inspection of this grouping shows that small permutations in the grasp configuration result in another grasp in the same group.
c) The mean of the absolute error for each joint in the original space between the predicted and target grasps is less than 20°. The error is the difference in $\vec{\theta}_{target\ grasp}$ and $\vec{\theta}_{predicted\ grasp}$. This indicates that for that specific subject, the two grasps are very

similar. This is how we account for unpredictable variations in grasp poses between subjects.

It should be noted that these criteria are purely for quantifying the prediction algorithm's performance and are entirely separate from the information used to generate the prediction.

The tuning parameters in Eqns. (8), (9), and (11) were set to yield acceptable results for all the subjects. Tuning these values individually for each subject would yield even better performance averages. For example, with minimal effort, an accuracy of approximately 90% was achieved for Subject 1 by choosing different values for these tuning parameters. To simplify the remaining discussions, the remainder of the results presented will be for Subject 1.

A simplified visualization of the simulation is presented in Fig. 2 with only three of the six principal component trajectories shown. The grasp convergence time, which is determined by the result of Eqn. (11) exceeding the defined threshold is 29.55%. The virtual time axis is the percentage of the motion completed. The noisy paths and their linear fits are shown as solid and dotted lines respectively. The results of Eqn. (8) are shown as well where the prediction line for the third principal component extends further behind those of the other principal components due to its decreased slope. The value of τ^+ from Eqn. (9) is shown to be very near the location in virtual time of the true grasp when all of the motion is complete.

In a review of Subject 1's performance in Fig. 3 it is clear that grasps 20 and 28 had worse performance than the other grasps. In Fig. 4, for the target grasp of 20 we see that the predicted grasps were 9, 14, 18, and 28. Grasp 18 and 28 have an average joint angle error (accuracy criterion (c)) of 13.25° and 23.55° respectively; therefore, grasp 28 falls just outside the acceptable window.

For the target grasp of 28, the two incorrect grasps, 9 and 33, have errors of 20.27° and 21.58° respectively which are also just outside the window. It is clear that the characterization of the accuracy of the grasp predicted is subject to the acceptable window and increasing its value only slightly increases the perceived accuracy.

Inspection of Eqn. (11) shows that an increased threshold, μ, should also yield an increased convergence time. Experimental evaluation verifies this relation. Choosing test values of 0.2, 0.4, and 0.6 result in convergence times of 20.21%, 32.39%, and 78.02% respectively. The resulting accuracies for all three values were ~90%. Too large of convergence time, as in the case of $\mu = 0.6$, effectively nullifies the prediction's utility as too much effort by the subject will be required.

For some of the grasps, the convergence of the algorithm towards a similar grasp is entirely intuitive. The motion towards Grasp 2, Small Cylinder, would theoretically pass through

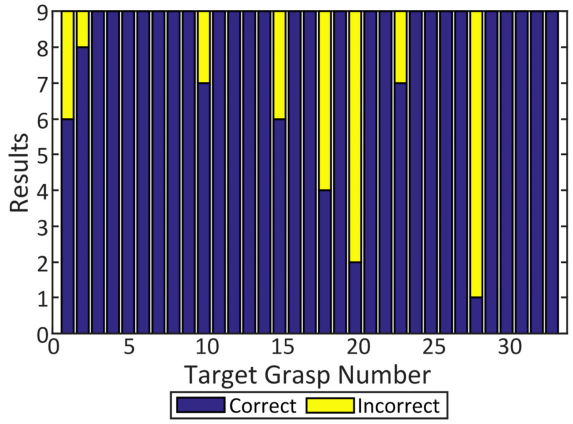

Figure 3: The results of the predictions made for each grasp with nine trials per grasp.

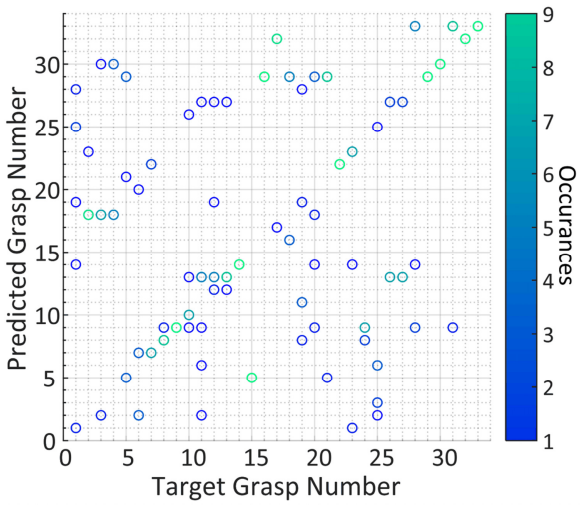

Figure 4: The target grasp and the resulting prediction from the algorithm.

Grasps 1 and 3, Large and Medium Cylinders, as well. In Fig. 6, this is confirmed when the configurations of Grasps 1 and 3 are almost exactly intersected by the motion towards Grasp 2. In the proposed controller that guides the user's motion based on the prediction, results like this are treated identically. Since the motion towards Grasp 2 naturally passes through Grasps 1 and 3, it is acceptable for the controller to also pass through these poses.

Alternatively, grasps in the Prismatic Small Stick and Sphere groups have very similar configurations when ignoring adduction, but the geometry they interact with is different as shown in Fig. 5. A strong example of this correlation is Grasp 6, Prismatic Four Finger, and Grasp 27, Quadpod. Results like these are also acceptable because the final configuration is so similar that the desired hand pose will be achieved regardless of the predicted grasp number.

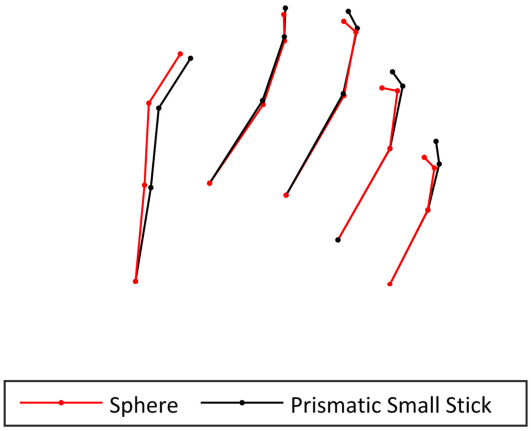

Figure 5: The pose for a four fingered grasp of a sphere (red) and small stick (black) without finger adduction.

To verify that the utilization of the reduced variables, instead of the original joint angles, in this prediction scheme yielded improved results, we implemented the algorithm directly on those joint angles. The results, for Subject 1, were an accuracy of 12.12% and convergence time of 36.91%, dramatically worse than those of the PCA driven algorithm. In addition to the improved performance, the equations for the prediction algorithm only need to be evaluated on the six principal components than all 16 individual joint angles.

4 PROPOSED CONTROLLER DESIGN AND FUTURE WORK

The functional requirements of a system in which the human operator and controlled system occupy the same space, such as with an exoskeletal glove, necessitate a means by which each system can physically influence the other to express their respective intents. An excellent strategy to achieve this is to make use of Series Elastic Actuators (SEA) to transmit force to the finger joints, such as in the Maestro [16], the work presented in [9], or our previous work and ongoing work presented in [17]. The user will be able to show their intended motion by deforming the elastic members in the SEAs and the glove will be able to precisely exert a force onto the user's hand to guide their motion.

In the facilitation of naturalistic hand movement, we propose the implementation of the prediction algorithm as the automation portion in a shifting Levels of Haptic Authority System [18]. To this end, the shift will be accomplished by

$$f_{out} = \nu f_{user} + \omega f_{\psi} \qquad (13)$$

where the force that the user physically exerts on the glove, f_{user}, is determined by the displacement of the elastic members on the SEAs. The force that guides the user towards the predicted grasp is f_{ψ}. The resulting force, f_{out}, is based on what both the user and prediction are trying to do. Upon the exertion of f_{out}, the prediction algorithm will iterate again and

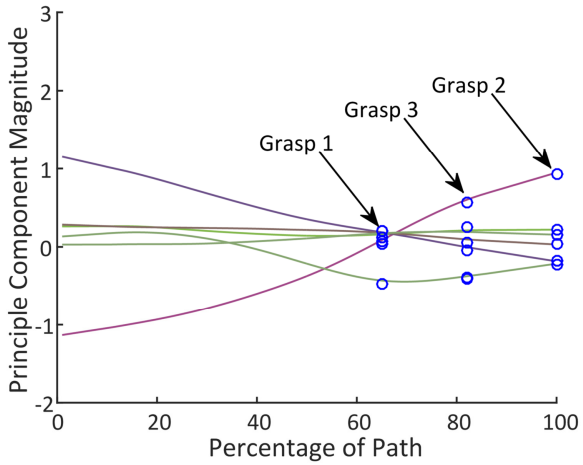

Figure 6: A noiseless trajectory for Grasp 2, small cylinder in the reduced variable space. The trajectory passes almost exactly through Grasps 1 and 3, Large and Medium Cylinder respectively.

f_{ψ} will update accordingly based on the new measure hand pose. The values of the user and glove authorities, ν and ω respectively, will initialize as 1 and 0 and approach 0 and 1 respectively as the time spent approaching a certain grasp configuration without being changed, via a new prediction, increases. This can be seen as a reversed implementation of the Look Ahead Guidance (LAG) system proposed in [19] in which the user takes the place of the autonomous controller and the path being followed is the updating prediction output. The LAG system is shown to have smooth transitions and haptic feedback to guide the user. We believe that this will help make the interaction between user and glove more comfortable. To further increase the synergy between the user and the glove, the value of ω can also be determined as a function of $\vec{c}(t)$ from Eqn. (11). This would help remove the delay between initial motion and the glove's assistance. As the prediction gains confidence, it applies more force on the user. The value of $\vec{c}(t)$ would naturally decrease if the user tries to move away from the predicted pose resulting in continuous adaptation.

5 CONCLUSION

This paper presents a novel grasp prediction algorithm using PCA and linear regression on noisy joint angle trajectories of the human hand. We propose that the use of this algorithm can guide the motion of an exoskeletal glove utilized for rehabilitation or assistance. By using six principal components to reduce the variable space from 16 dimensions to six dimensions and implementing a novel grasp selection equation, the algorithm was able to achieve markedly improved results. The grasp prediction accuracy was improved by approximately fivefold by using the latent variable space as compared to using the full dimensionality data. Additionally, a new functional and geometric grasp grouping was developed to aid in the qualification of the algorithm. Since the algorithm

was tested on existing data with known time steps, we developed a dynamic look-ahead function to estimate the point in the time at which the grasp would be completed despite the nonlinear and nonuniform trajectories of the grasps in this data set. Furthermore, the algorithm is able to provide temporally significant results, often predicting intermediate grasping positions to aid the user on their way to their desired pose.

We believe that this prediction algorithm has the capability to drastically improve the dexterity, and therefore utility, of hand orthotics. The prediction algorithm implemented on a dexterous glove provides a means by which a user with limited mobility can still perform complex hand movements that increase their ability to perform ADLs. We would like to execute this implementation on a highly flexible glove that makes use of SEAs to provide smooth, force-based assistance to an impaired operator.

ACKNOWLEDGMENTS

The authors are grateful to Adam Williams and Bijo Sebastian for their assistance during the development of this work.

REFERENCES

[1] Lin, J., Wu, Y., and Huang, T. S., 2000. "Modeling the Constraints of Human Hand Motion". *Constraints*, pp. 121– 126.

[2] Santello, M., Flanders, M., and Soechting, J. F., 1998. "Postural hand synergies for tool use". *The Journal of Neuroscience, 18*(23), pp. 10105–10115.

[3] Romero, J., Feix, T., Kjellstrom, H., and Kragic, D., 2010. "Spatio-temporal modelling of grasping actions". *Proc. IEEE/RSJ International Conference on Intelligent Robots and Systems*, pp. 2103–2108.

[4] Feix, T., Romero, J., Schmiedmayer, H. B., Dollar, A. M., and Kragic, D., 2016. "The GRASP Taxonomy of Human Grasp Types". *IEEE Transactions on Human-Machine Systems*.

[5] Ciocarlie, M., Goldfeder, C., and Allen, P., 2007. "Dexterous grasping via eigengrasps: A low-dimensional approach to a high-complexity problem". *Proceedings of the Robotics: Science & Systems 2007 Workshop-Sensing and Adapting to the Real World, Electronically published*.

[6] Matrone, G. C., Cipriani, C., Secco, E. L., Magenes, G., and Carrozza, M. C., 2010. "Principal components analysis based control of a multi-dof underactuated prosthetic hand". *Journal of NeuroEngineering and Rehabilitation, 7*(1), pp. 1–13.

[7] Arata, J., Ohmoto, K., Gassert, R., Lambercy, O., Fujimoto, H., and Wada, I., 2013. "A new hand exoskeleton device for rehabilitation using a three-layered sliding spring mechanism". *Proceedings - IEEE International Conference on Robotics and Automation*, pp. 3902–3907.

[8] Nycz, C. J., Delph, M. A., and Fischer, G. S., 2015. "Modeling and design of a tendon actuated soft robotic exoskeleton for hemiparetic upper limb rehabilitation". *Proceedings of the Annual International Conference of the IEEE Engineering in Medicine and Biology Society, EMBS, 2015Novem*, pp. 3889–3892.

[9] Jo, I., and Bae, J., 2017. "Design and control of a wearable and force-controllable hand exoskeleton system". *Mechatronics, 41*, 2, pp. 90–101.

[10] Liu, M., and Xiong, C., 2014. "Synergistic Characteristic of Human Hand during Grasping Tasks in Daily Life". pp. 67– 76.

[11] Ingram, J. N., and Wolpert, D. M., 2009. "UKPMC Funders Group The statistics of natural hand movements". *Brain, 188*(2), pp. 223–236.

[12] Zhang, L., Dong, W., Zhang, D., and Shi, G., 2010. "Twostage image denoising by principal component analysis
with local pixel grouping". *Pattern Recognition, 43*(4), 4, pp. 1531–1549.

[13] Shlens, J., 2009. "A Tutorial on Principal Component Analysis" from https://arxiv.org/abs/1404.1100.

[14] Liu M-J, Xiong C-H, X. L. H. X.-L., 2016. HUST Dataset from http://www.handcorpus.org/?p=1596.

[15] Feix, T., Pawlik, R., Schmiedmayer, H.-B., Romero, J., and Kragi, D., 2009. "A comprehensive grasp taxonomy". *Robotics, Science and Systems Conference: Workshop on Understanding the Human Hand for Advancing Robotic Manipulation*, pp. 2–3.

[16] Yun, Y., Dancausse, S., Esmatloo, P., Serrato, A., Merring, C. A., and Deshpande, A. D. "An EMG-Driven Assistive Hand Exoskeleton for Spinal Cord Injury Patients: Maestro".

[17] Refour, E., Sebastian, B., and Ben-Tzvi, P., 2018. "Two-Digit Robotic Exoskeleton Glove Mechanism: Design and Integration". *Journal of Mechanisms and Robotics, 10*(2), p. 025002.

[18] Abbink, D. A., Mulder, M., and Boer, E. R. "Haptic shared control: smoothly shifting control authority?".

[19] Forsyth, B. A., and MacLean, K. E., 2006. "Predictive Haptic Guidance: Intelligent User Assistance for the Control of Dynamic Tasks". *IEEE Transactions on Visualization and Computer Graphics, 12*(1), pp. 103–113.